

Surface Roughness Measurement of Machined Surfaces by Machine Vision Technique

P.Naresh, Syed Altaf Hussain, B. Durga Prasad

Abstract: Aluminium material is extremely used in many manufacturing industry sectors, there are several uses of aluminium, i.e., formability, high strength, thermal resistance, flexibility and high resistance towards corrosion. The advantages in different engineering fields demand various machining operations to be performed on metal matrix composites (MMCs). In the present investigation, the machine vision technique is used to observe roughness of surface in turning of MMCs composites. The process parameters considered are weight percentage of titanium carbide, feed, cutting speed and depth of cut. Experiments are planned and executed according to central composite design technique on all geared lathe machine using TiCN-Al₂O₃ tool insert. During machining operation the machining surfaces are captured through machine vision technique. A program is written in MATLAB which is used to analyze G_a values for bitmap of captured images and stylus probe instrument is used to estimate surface finish of machined surfaces.

Index Terms: Central composite design, Machining, Machine vision technique, Surface roughness

I. INTRODUCTION

AA7068 is light weight material and good mechanical properties, i.e., hardness, corrosion resistance, good thermal and electrical conductivity, fatigue, wear resistance and superior properties for aluminium and its alloys have been used in versatile engineering applications such as automobiles, aircrafts, railway cars, mineral processing sectors, marine vessels and showing interest towards the major quality components in respect of tolerances and surface finish [1-5]. The surface roughness evaluation is very important role in various design fields such as contact deformation, friction, positional accuracy, heat and electrical current conduction, tightness of the joints. Therefore, surface roughness has been the theoretical and experimental investigations for many years.

Various techniques are developed for measuring surface roughness for machined specimens ranging from simple stylus probe instrument to sophisticated optical techniques. Hence the Al based MMCs are the most sought after material in various [6]. Basically, surface roughness measurements are generally categorized into two parts: contact and noncontact methods. The stylus probe instrument is direct contact method, which uncontrollable scratches the machined surfaces of the objectives and controls the efficiency, low

accuracy of specimens wouldn't meet requirements related to various sectors [7-9]. Different optical metrology methods are used to resolve surface roughness problems such as coherence scanning interferometer, focus variation instruments, chromatic con-focal microscopy, and phase shifting inter-ferometry has been developed [10]. However, due to the inconvenient operation, high accuracy, high investment and effects on the environment, the uses of these noncontact methods are limited [11, 12].

In machine vision technique have various advantages, such as high accuracy, high speed measurement, low cost and flexibility, high information, and non-contact mode, Moreover this technique is used in industrial uses are detect the local defected area which is complicated to estimate conventionally. Because of these uses, the machine vision technique is used to evaluation surface finish of various components, such as leaf, fabric, ceramics, and film capacitors, not only a mechanical parts [13-18]. Machine vision method is based machined surface quality measurement technology moreover consists of contact mechanism analysis, pre-processing algorithm design, image based-indices design, roughness prediction algorithm design, and experimental design [19-30]. From the majority of designs the image-based design on the information of gray scale image [31]. From these drawbacks the direct contact technique are not suitable for high-speed industrial inspection.

From past investigators using machine-vision method for surface roughness assessment have various deliberate parameters, with stylus probe instrument of average surface finish performed on the same surface. Kumar et al. [32] adopted a machine vision technique to observed machined surface images and calculate the surface finish by regression equation. The values of average G_a are calibrated with respect to Ra of the surface which is taken by the stylus. Hoy & Yu [33]. reported a 2D-FFT measurement parameter of the surface roughness. Manjunatha, et.al. observed the surface finish using machine vision the surface parameter. They applied geometric search approach to the average gray scale values (G_a) to enhance the surface roughness. CCD camera is used to acquire the images of machined surfaces later pre-processor was done to eliminate effects causes to improper illumination and noise. Median low pass filter was used to the captured images to avoid the salt and pepper effect [34-35]. Hatem El-Ghandoor, et al. observed the various aluminium surface finishes and its digital speckle images using Charge Coupled Device (CCD) camera. As per results, surface finish is depending on degree of agglomeration of the speckle images [36].

Revised Manuscript Received on December 22, 2018.

P. Naresh, Research Scholar, Department of Mechanical Engineering, Jawaharlal Nehru Technological University Anantapur, Ananthapuramu, Andhra Pradesh, INDIA.

Syed Altaf Hussain, Professor, Department of Mechanical Engineering Rajeev Gandhi Memorial College of Engineering & Technology, Nandyal, Andhra Pradesh, INDIA.

B. Durga Prasad, Professor, Department of Mechanical Engineering, Jawaharlal Nehru Technological University Anantapur, Ananthapuramu, Andhra Pradesh, INDIA.



Luk et al. [37] used mathematical parameters, stylus method is used to calculate the surface roughness and find grey intensity histogram and correlated with Ra. Kocer, et al. [38] observed the relationship between R_a and G_a . Lee, et.al [39, 40] developed a work-piece profile acquisition method using 2D-FFT and image processing. In this present work, metal matrix composites specimens are machined using all geared lathe by tool TiCN- Al_2O_3 . Central Composite Design is used for the experimentation. During machining process the image surfaces are captured by using a machine vision system. A program is developed in MATLAB to estimate average grey scale values (G_a) for the captured surfaces and surface finish (R_a) values were measured conventionally.

II. EXPERIMENTATION

In present investigation, Al7068/TiC materials are fabricated using stir casting at various weight fraction of reinforcement varied from 0 to 10 wt. % in steps of 2wt.%. The test specimens are prepared with a diameter of 22 mm and length 190 mm respectively. The fabricated specimens are machined in a Kirloskar made turnmaster-35 lathe with a attachment of machine vision system which consists of WATEC 902B1/2" charge coupled device monochrome camera with CCIR a schematic diagram as shown in Fig. 1. Fabricated specimens are machined in Kirloskar all geared lathe of model 9857B and charge amplifier model was 5070A specifications of tool holder are PSB NR-2525M12 and the cutting tool is TiCN- Al_2O_3 made by the kenna metals and tool insert is SNMG120408 and experimental setup is shown in Fig. 2. The TiCN- Al_2O_3 tools are especially wear resistance collate to ceramic tools or tungsten carbide tools. Experiments are executed as per central composite design [41] and different surface textures were obtained for different parameters at machining operation. An easy way to comply with the paper formatting requirements is to use this document as a template and simply type your text into it. Your paper must use a page size corresponding to A4 which is 21cm wide and 29.7cm long. The margins must be set as follows:

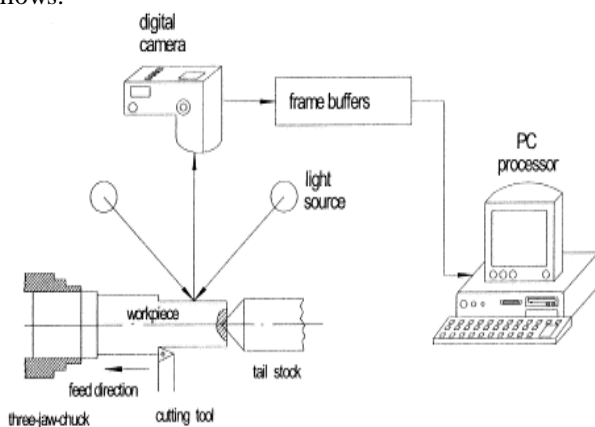


Fig.1: Layout of a machine vision system

Table 1: Control parameters and their levels

S.No	Levels/ Parameters	-2	-1	0	1	2
1	Weight	2	4	6	8	10

		percentage of TiC, (wt.%)				
2	Cutting Speed (V), m/min,	30	40	50	60	70
3	Feed (f), mm/rev	0.06	0.07	0.08	0.09	0.1
4	Depth of Cut (d), mm	0.2	0.5	0.8	1.1	1.4



Fig.2: Experimental Setup for machining operation

In the present experiment four variables are considered to measure surface roughness viz., $a_1, a_2, a_3,$ and a_4 and the experiments are conducted as per developed design. The value of α is 2 is selected as per design and plan consists of 2^4 factorial designs, 8 star points and 7 central points. The identified independent control parameters are: wt. % of TiC, V, f, and d. for various control parameters and their level, notation are given in Table 1. The various control parameters and estimated responses of roughness of surface (R_a) for 31 runs are mentioned in Table 2.

The machined surfaces have recorded by using CCD camera for 31 experiments. The captured profiles were started in a bitmap and analyzed the G_a values with a program developed in MATLAB. The surface finish (R_a) of the machined surfaces is calculated theoretically by surface roughness tester

The arithmetic average of peaks of surface unevenness observed from the mean values calculated.

$$R_a = \frac{1}{n} \sum_{i=1}^n y_i \quad (1)$$

R_a arithmetic average roughness, y_i height of irregularities of the roughness, and n sampling data.

In a case the vision system G_a is used to estimate roughness. The arithmetic average gray scale values and is expressed as

$$G_a = \frac{1}{n} \sum_{i=1}^n g_i \quad (2)$$

Where arithmetic average gray scale values g_i is difference between individual pixels and gray scale intensity, in the captured images and average gray values of all the pixels are taken into consideration.

III. SURFACE ROUGHNESS

The important aspect of roughness measurement is to extract the surface finish parameters of machined surfaces observed from machine vision system. Surface finish is estimated based on spectral frequency in the 2D Fourier transform (Fz) domain in order to detect texture periodicities. A mechanism of 2D Fourier transform is shown in Fig. 3. [42] and [43]. The F_2 shows the characterization of the captured surfaces in terms of frequency constituent [44]. Huaianet al, Liu et al. and Sarma et al. [45-47] have investigated a set of 31 texture features in the spectral frequency domain. In this investigation the vision system is adopted to estimate the surface roughness of MMC composite specimens.

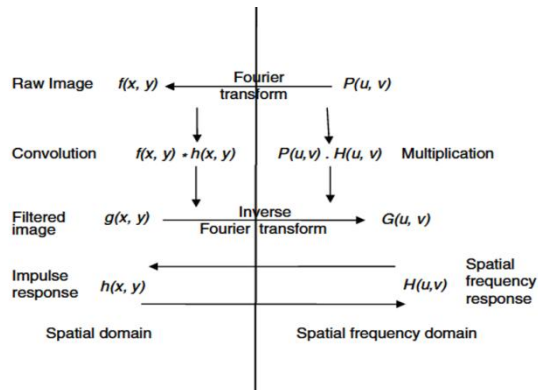


Fig. 3: Two dimensional Fourier transforms definition [42 and 43]

Let $f(x, y)$ is Ga of a pixel at (x, y) is an actual size of images N_x, N_y pixels. The discrete 2DFT [23] of $f(x, y)$ is given by:

$$F(u, v) = \frac{1}{N} \sum_{x=0}^{N-1} \sum_{y=0}^{N-1} f(x, y) \cdot \exp[-j2\pi(ux + vy) / N] \quad (3)$$

For

$$u, v = 0, 1, 2, 3, 4, 5, 6, \dots, N-1 \quad (4)$$

The 2DFT is generally i.e.:

$$F(u, v) = R(u, v) + jI(u, v) \quad (5)$$

where $R(u, v)$ -imaginary components of $F(u, v)$ & $jI(u, v)$ -real components of $F(u, v)$

The Fourier spectrum $|F(u, v)|$ phase $\Phi(u, v)$ and power spectrum $P(u, v)$ are defined by

$$|F(u, v)| = [R^2(u, v) + I^2(u, v)]^{1/2} \quad (6)$$

$$\Phi(u, v) = \tan^{-1} \frac{I(u, v)}{R(u, v)} \quad (7)$$

$$P(u, v) = |F(u, v)|^2 = R^2(u, v) + I^2(u, v) \quad (8)$$

The machine surface images at various cutting speeds and corresponding PSD images are shown in Fig. 4 and 5. PSD describes how the variance of a time series is appropriated with frequency.

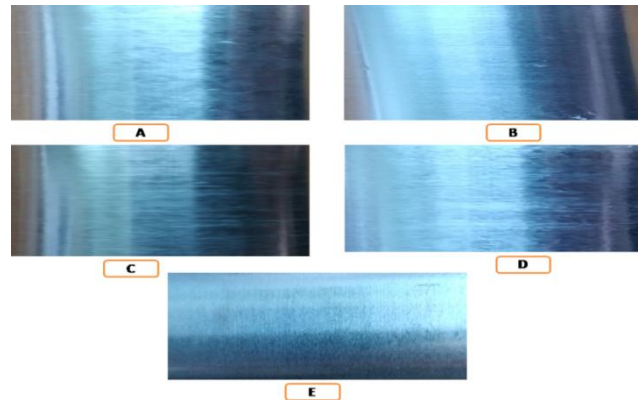


Fig. 4: Captured surface taken at (A) 30m/min, (B) 40m/min, (C) 50m/min, (D) 60m/min and (E) 70m/min.

IV. RESULTS & DISCUSSION

Table 2: Experimental results for surface roughness

S.No	Coded Variables				Un coded Variables				Surface roughness, Ra μm
	a1	a2	a3	a4	Wt. % of TiC	V m/min	f mm/rev	d mm	
1	-	-	-	-	4	40	0.07	0.5	0.553
2	1	-	-	-	8	40	0.07	0.5	0.652
3	-	1	-	-	4	60	0.07	0.5	0.483
4	1	1	-	-	8	60	0.07	0.5	0.609
5	-	-	1	-	4	40	0.09	0.5	0.596
6	1	-	1	-	8	40	0.09	0.5	0.689
7	-	1	1	-	4	60	0.09	0.5	0.452
8	1	1	1	-	8	60	0.09	0.5	0.566
9	-	-	-	1	4	40	0.07	1.1	0.468
10	1	-	-	1	8	40	0.07	1.1	0.556
11	-	1	-	1	4	60	0.07	1.1	0.549
12	1	1	-	1	8	60	0.07	1.1	0.675
13	-	-	1	1	4	40	0.09	1.1	0.572
14	1	-	1	1	8	40	0.09	1.1	0.673
15	-	1	1	1	4	60	0.09	1.1	0.585
16	1	1	1	1	8	60	0.09	1.1	0.678
17	-	0	0	0	2	50	0.08	0.8	0.397
18	2	0	0	0	10	50	0.08	0.8	0.726
19	0	2	0	0	6	30	0.08	0.8	0.661
20	0	2	0	0	6	70	0.08	0.8	0.556
21	0	0	-	0	6	50	0.06	0.8	0.523
22	0	0	2	0	6	50	0.10	0.8	0.650
23	0	0	0	-	6	50	0.08	0.2	0.499



24	0	0	0	2	6	50	0.08	1.4	0.619
25	0	0	0	0	6	50	0.08	0.8	0.621
26	0	0	0	0	6	50	0.08	0.8	0.645
27	0	0	0	0	6	50	0.08	0.8	0.654
28	0	0	0	0	6	50	0.08	0.8	0.653
29	0	0	0	0	6	50	0.08	0.8	0.612
30	0	0	0	0	6	50	0.08	0.8	0.626
31	0	0	0	0	6	50	0.08	0.8	0.639

The estimated values of surface roughness using Fourier transform are presented. The experimental runs as per CCD is as shown in Table 2, surface finish images are captured by charge coupled device camera for each experimental run. The recorded surfaces are evaluated for gray scale values to find the avg. G_a values and PSD graphs are obtained for 31 captured images. The R_a values are acquired for various cutting parameters are listed in Table 2. Also, the comparison plot of estimated for surface roughness values using stylus approach and vision approach in Fig. 6. And a comparison graph in between experimental values and predicted values is shown Fig. 7. From Fig. 5, Sample PSD graphs is explained that, as cutting speeds increases the PSD decreases, which indicates improved the surface roughness. The results obtained indicate the superiority of the 2DFT method over other schemes. The experimental results reveals are analyzed using RSM and the below equation has been developed for surface roughness (R_a) in coded units given as:

$$R_a = -0.815 + 0.0880 * Wt.\% + 0.00902 * V + 26.76 * f - 0.677 * d - 0.00437 * Wt.\% * Wt.\% - 0.000057 * V * V - 112.2 * f * f - 0.2011 * d * d + 0.000212 * Wt.\% * V - 0.150 * Wt.\% * f - 0.0035 * Wt.\% * d - 0.2037 * V * f + 0.01267 * V * d + 5.50 * f * d$$

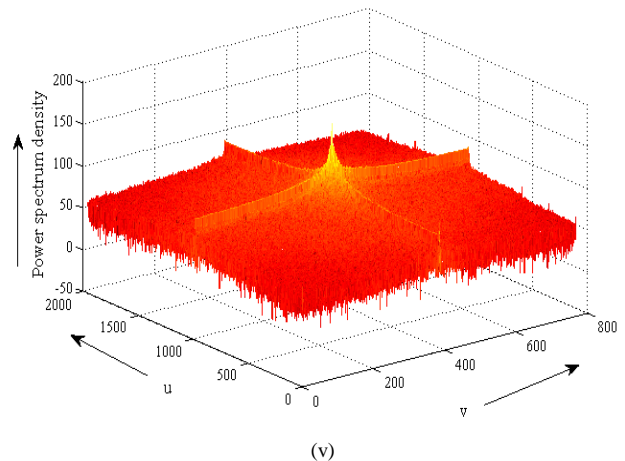
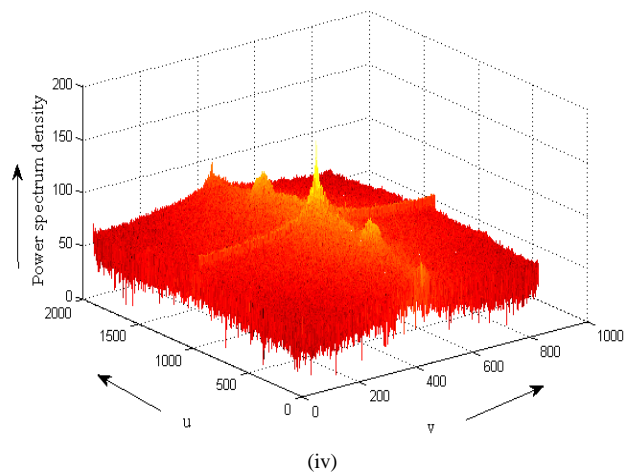
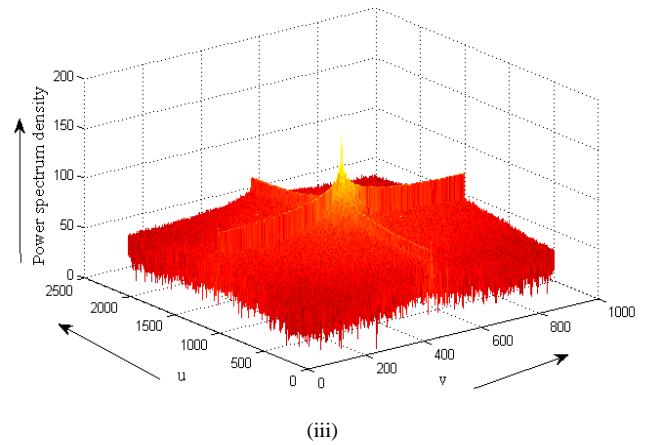
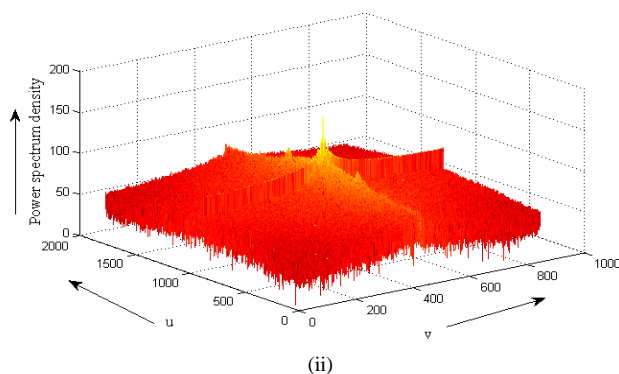
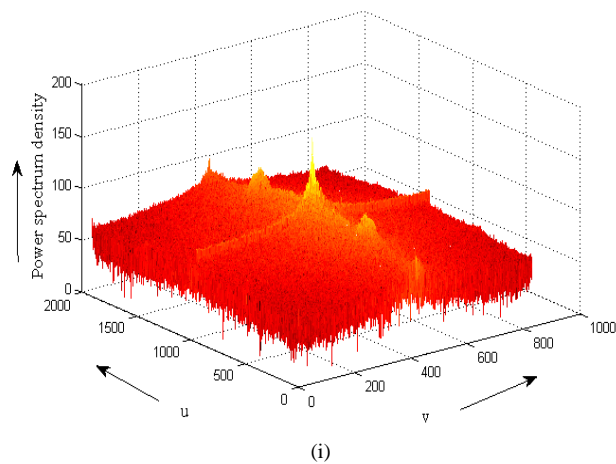


Fig. 5: PSD graphs for different cutting speeds of (i) 54 m/min, (ii) 82 m/min, (iii) 126 m/min, (iv) 194 m/min and (v) 302 m/min

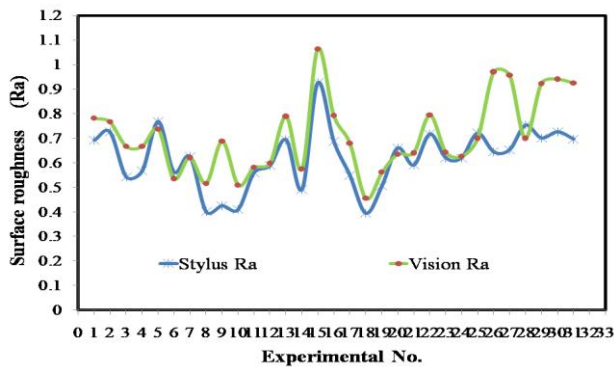


Fig. 6: Analogy of stylus approach and vision approach

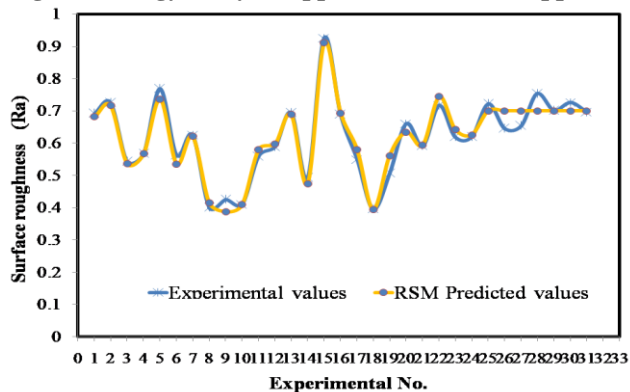


Fig. 7: Analogy of observed values and expected values for surface roughness.

V. CONCLUSION

Present work clearly concluded that the surface roughness is calculated for machined specimen using stylus probe instrument and machine vision technique. Machine vision technique is highly effective for measurement of machined specimens, as it is non-contact and reliable technique. It can be concluded as machine vision technique has average accuracy and provides best tolerances.

REFERENCES

1. Shin, J.; Kim, T.; Kim, D.; Kim, D.; Kim, K. Castability and Mechanical Properties of New 7xxx Aluminum Alloys for Automotive Chassis/body Applications. *J. Alloy. Compd*, 698, 577–590, 2017.
2. Ashraf, P.M.; Shibli, S.M.A. Development of Cerium Oxide and Nickel Oxide-Incorporated Aluminium Matrix for Marine Applications. *J. Alloy. Compd*, 484, 477–482, 2009.
3. Cerik, B.C. Damage Assessment of Marine Grade Aluminium Alloy-Plated Structures due to Air Blast and Explosive Loads. *Thin-walled Struct*, 110, 123–132, 2017.
4. Teimouri, R.; Amini, S.; Mohagheghian, N. Experimental Study and Empirical Analysis on Effect of Ultrasonic Vibration during Rotary Turning of Aluminum 7075 Aerospace Alloy. *J. Manuf. Process*, 26, 1–12, 2017.
5. Heinz, A.; Haszler, A.; Keidel, C.; Moldenhauer, S.; Benedictus, R.; Miller, W.S. Recent Development in Aluminium Alloys for Aerospace Applications. *Mater. Sci. Eng. A*, 280, 102–107, 2000.
6. K.Rajkumar, P.Rajan and J. Marian Antony Charles, *Procedia Engineering*, vol 86, pp 34-41, 2014.
7. Lee BY, Juan H, Yu SF. A study of computer vision for measuring surface roughness in the turning process. *Int J Adv Manuf Technol*, 19(4):295–301, 2009.
8. Shahabi HH, Ratnam MM. Prediction of surface roughness and dimensional deviation of workpiece in turning: a machine vision approach. *Int J Adv Manuf Technol*, 48(1–4):213–26, 2010.
9. Kiran MB, Ramamoorthy B, Radhakrishnan V. Evaluation of surface roughness by vision system. *Int J Mach Tool Manufact*, 38(5–6):685–90, 1998.

10. Su R, Wang Y, Coupland J, Leach RK. On tilt and curvature dependent errors and the calibration of coherence scanning interferometry. *Optic Express*, 25(4): 3297–310, 2017.
11. Yilbas Z, Hasmi MSJ. Surface roughness measurement using an optical system. *J Mater Process Technol*, 88(1–3):10–22, 1999.
12. Leach RK. *Optical measurement of surface topography*. Springer; 2011.
13. Sutton MA, Orteu JJ, Schreier H. *Image correlation for shape, motion and deformation measurements: basic concepts, theory and applications*. New York: Springer Science & Business Media; 2009.
14. Hladnik A, Lazar M. Paper and board surface roughness characterization using laser profilometry and gray level cooccurrence matrix. *Nord Pulp Pap Res J*, 26(1): 99–105, 2011.
15. Yang Y, Zha Z, Gao M, He Z. A robust vision inspection system for detecting surface defects of film capacitors. *Signal Process*, 124(C):54–62, 2016.
16. Tholt B, Miranda-Júnior WG, Prioli R, Thompson J, Odae M. Surface roughness in ceramics with different finishing techniques using atomic force microscope and profilometer. *Operat Dent*, 31(4):442–9, 2006.
17. Bediaf H, Sabre R, Journaux L, Cointault F. Comparison of leaf surface roughness analysis methods by sensitivity to noise analysis. *Biosyst Eng* 2015; 136:77–86. Wang X, Georganas ND, Petriu EM. Fabric texture analysis using computer vision techniques. *IEEE Trans Instrum Meas* 60(1):44–56, 2011.
18. Kumar BM, Ratnam MM. Machine vision method for non-contact measurement of surface roughness of a rotating workpiece. *Sens Rev*, 35(1):10–9, 2015.
19. Vorburger TV, Marx E, Lettieri TR. Regimes of surface roughness measurable with light scattering. *Appl Optic* 1993; 32(19):3401–8.
20. Maradudin AA. *Light scattering and nanoscale surface roughness*. New York: Springer; 2007.
21. Dhanasekar B, Mohan NK, Bhaduri B, Ramamoorthy B. Evaluation of surface roughness based on monochromatic speckle correlation using image processing. *Precis Eng*, 32(3):196–206, 2008.
22. Palani S, Natarajan U. Prediction of surface roughness in CNC end milling by machine vision system using artificial neural network based on 2D Fourier transform. *Int J Adv Manuf Technol*, 54(9–12):1033–42, 2011.
23. Dhanasekar B, Ramamoorthy B. Digital speckle interferometry for assessment of surface roughness. *Optic Laser Eng*, 46(3):272–80, 2008.
24. Dhanasekar B, Ramamoorthy B. Assessment of surface roughness based on super resolution reconstruction algorithm. *Int J Adv Manuf Technol* 35(11): 1191–205, 2008.
25. Dhanasekar B, Ramamoorthy B. Restoration of blurred images for surface roughness evaluation using machine vision. *Tribol Int*, 43(1–2):268–76, 2010.
26. Priya P, Ramamoorthy B. The influence of component inclination on surface finish evaluation using digital image processing. *Int J Mach Tool Manufact*, 47(3): 570–9, 2007.
27. Jeyapoovan T, Murugan M. Surface roughness classification using image processing. *Measurement*, 46(7):2065–72, 2013.
28. Yang SH, Natarajan U, Sekar M, Palani S. Prediction of surface roughness in turning operations by computer vision using neural network trained by differential evolution algorithm. *Int J Adv Manuf Technol*; 51(9):965–71, 2010
29. Palani S, Natarajan U, Chellamalai M. On-line prediction of micro-turning multiresponse variables by machine vision system using adaptive neuro-fuzzy inference system (ANFIS), 24(1):19–32, 2013.
30. Guo R, Tao Z. A study of neural network for surface characteristics in-process optical measurement. *Optik (Stuttg.)*; 124(17):2821–4, 2013.
31. Zhang J, Tan T. Brief review of invariant texture analysis methods. *Pattern Recogn*; 35(3):735–47, 2002.
32. R. Kumar, P. Kulashekar, B. Dhanasekar, B. Ramamoorthy, Application of digital image magnification for surface roughness evaluation using machine vision, *International Journal of Machine Tools & Manufacture* 228–234, 45, 2005.
33. D.E.P. Hoy, F. Yu. Surface quality assessment using computer vision methods, *Journal of Materials Processing Technology*. 28 (1-2): 265-274, 1991.
34. Manjunatha, Dr R Rajashekar, Dr B M Rajaprakash, Naveen S, Mohan G. Evaluation of Surface Roughness of Machined Components using Machine Vision Technique. *International Journal of Engineering Development and Research*. Volume 5, Issue 4 ISSN: 2321-9939, 2017.

35. J. Darani Priya, J. Mahashar Ali. 2015. Design of a Measurement System for Surface Roughness using Speckle Images. International Journal of Advance Engineering and Research Development. Volume 2, Issue 4 pp300-305, 2015.
36. Hatem El-Ghandoor, Mohamed Saady and Ahmed Ashour, Analysis of Surface Roughness Using Laser Optical Imaging Techniques. Journal of Materials Science and Engineering B 2 (1), 7-15, 2012.
37. F. Luk, V. Hyunh and W. North, Measurement of Surface Roughness by a Machine Vision System, Journal of Physics E Scientific Instruments 22, 977-980, 1989.
38. Koçer, E.; Horozoglu, E. Asiltürk, I. Noncontact surface roughness measurement using a vision system. Proc. SPIE Int. Soc. Opt. Eng., 9445, 944525, 2015.
39. Lee, W.K.; Ratnam, M.M.; Ahmad, Z.A. Detection of fracture in ceramic cutting tools from workpiece profile signature using image processing and fast Fourier transform. Precis. Eng., 44, 131–142, 2015.
40. Lee, W.K.; Ratnam, M.M.; Ahmad, Z.A. Detection of chipping in ceramic cutting inserts from workpiece profile during turning using fast Fourier transform (FFT) and continuous wavelet transform (CWT). Precis. Eng., 47, 406–423, 2017.
41. W.G. Cochran, G.M.Cox. Experimental design. India. Asia publishing house. 1963.
42. Awcock, G. J. and Thomas, R. Applied Image Processing, Macmillan Press, Basingstoke, Hampshire, London. 1995.
43. Sarma P.M.M, Karunamoorthy L. Palani Kumar. K. Surface Roughness Parameters Evaluation in Machining GFRP Composites by PCD Tool using Digital Image Processing. Journal of Reinforced Plastics and Composites, vol. 00, No./2008. 1-20. [http://dx.: 1doi0.1177/0731684408089858](http://dx.doi.org/10.1177/0731684408089858). 2008.
44. Du-Ming Tsai and Jong-Jong Chen. A Vision System for Surface Roughness Assessment using Neural Networks, International Journal of Advanced Manufacturing Technology, 14(6): 412–422. 1998.
45. Song-Sheng Liu and Jernigan, M. E. Texture Analysis and Discrimination in Additive Noise, Computer Vision, Graphics and Image Processing, 49: 52–67. 1990.
46. Huaian Yi, Jian Liu, Peng Ao, Enhui Lu, and Hang Zhang. Visual Method For Measuring The Roughness of a Grinding Piece Based on Colour Indices. Optics Express 17215. vol. 24, no.15 -25. <http://dx.doi.org/10.1364/OE.24.017215>. 2016.
47. Sarma P.M.M, Karunamoorthy L. Palani Kumar. K. Surface Roughness Parameters Evaluation in Machining GFRP Composites by PCD Tool using Digital Image Processing. Journal of Reinforced Plastics and Composites, vol. 00, No./2008. 1-20. <http://dx.: 1doi0.1177/0731684408089858>. 2008.